Analytica Chimica Acta 1189 (2022) 339206

Contents lists available at ScienceDirect

Analytica Chimica Acta

journal homepage: www.elsevier.com/locate/aca

Aptamers targeting a tumor-associated extracellular matrix component: The human mature collagen XIα1

Ramón Lorenzo-Gómez [a, b], Rebeca Miranda-Castro [a, b], Juan R. de los Toyos [b, c], Noemí de-los-Santos-Álvarez [a, b, *], María Jesús Lobo-Castañón [a, b, **]

[a] Departamento de Química Física y Analítica, Facultad de Química, Universidad de Oviedo, Av. Julián Clavería 8, 33006, Oviedo, Spain
[b] Instituto de Investigación Sanitaria del Principado de Asturias, Avenida de Roma, 33011, Oviedo, Spain
[c] Departamento de Inmunología, Facultad de Medicina y Ciencias de La Salud, Universidad de Oviedo, Av. Julián Clavería 6, 33006, Oviedo, Spain

HIGHLIGHTS

- Extracellular matrix components are an understudied source of cancer biomarkers.
- Detection of collagen XI, overexpressed in some cancers, needs suitable probes.
- A 16mer peptide was the target for the first aptamer for α chain of human collagen XI.
- Mass spectrometry verifies collagen XI as the target of D1 aptamer from cell lysates.
- Antibody-aptamer sandwich assay detects colXIα1 in cell lysates.

GRAPHICAL ABSTRACT

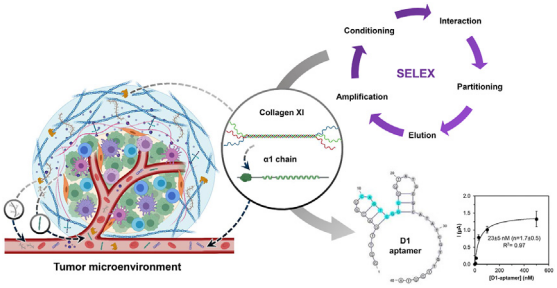

ARTICLE INFO

Article history:
Received 28 July 2021
Received in revised form
16 October 2021
Accepted 19 October 2021
Available online 21 October 2021

Keywords:
Human collagen XI alpha 1 chain
Aptamer
SELEX
Electrochemical characterization
Neoepitope

ABSTRACT

The extracellular matrix (ECM) plays an essential role in tumor progression and invasion through its continuous remodeling. The growth of most carcinomas is associated with an excessive collagen deposition that provides the proper environment for tumor development and chemoresistance. The α1 chain of a minor human collagen, type XI, is overexpressed in some tumor stroma, but not found in normal stroma. To test the clinical utility of this collagen as a cancer biomarker, specific receptors are needed. Available antibodies do not show enough selectivity or are directed toward the propeptide region that is cleaved when the protein is released to the ECM. Here we show the selection of an aptamer for the specific C-telopeptide region using a 16-mer peptide as the target for the SELEX. The aptamer selected with a K_d of ~25 nM was able to capture the collagen XI from cell lysates. It was also used for target detection in a mixed antibody-aptamer sandwich assay showing it can be useful for diagnostic purposes in biological fluids.

* Corresponding author. Departamento de Química Física y Analítica, Facultad de Química, Universidad de Oviedo, Av. Julián Clavería 8, 33006, Oviedo, Spain.
** Corresponding author. Departamento de Química Física y Analítica, Facultad de Química, Universidad de Oviedo, Av. Julián Clavería 8, 33006, Oviedo, Spain.
E-mail addresses: ramonlorenzogomez@gmail.com (R. Lorenzo-Gómez), mirandarebeca@uniovi.es (R. Miranda-Castro), jrtoyos@uniovi.es (J.R. de los Toyos), santosnoemi@uniovi.es (N. de-los-Santos-Álvarez), mjlc@uniovi.es (M.J. Lobo-Castañón).

https://doi.org/10.1016/j.aca.2021.339206

Abbreviation list

16mer	16-amino acid peptide from collagen XIα1 used as SELEX target
16mer-MBs	streptavidin-coated magnetic beads modified with biotinylated 16mer
antiF-POD	anti-fluorescein Fab-peroxidase
colXIα1	alpha 1 chain of collagen XI
BSA	bovine serum albumin
BSA-T-MBs	tosylactivated magnetic beads modified with BSA
BSA-16mer-T-MBs	tosylactivated magnetic beads modified with 16mer-BSA conjugate
C-MBs	carboxylated magnetic beads
ECM	extracellular matrix
EMT	epithelial-to-mesenchymal transition
FBS	fetal bovine serum
MBs	magnetic beads
NC	non-collagenous
PDAC	pancreatic ductal adenocarcinoma
RT	room temperature
SELEX	systematic evolution of ligands by exponential enrichment
strep-MBs	streptavidin-coated magnetic beads
strep-POD	streptavidin-peroxidase
TBE	Tris-Borate-EDTA

1. Introduction

Liquid biopsy, as a subrogate of tissue, is rapidly emerging as a tool to monitor tumor evolution almost in real time [1], providing the basis for individualized treatments. In cancer management, adoption of this approach shifts the focus from organ to biomarkers shed by the tumor cells into the body fluids. Circulating tumor cells and DNA are the currently approved biomarkers for liquid biopsy diagnostics [1,2].

Solid tumors include a tumor microenvironment that can also be a source of biomarkers for liquid biopsy. They comprise stromal and immune cells, blood vessels and the extracellular matrix (ECM) [3]. ECM is the scaffold that provides mechanical support to all organs, tissues and individual cells through a three-dimensional network of highly cross-linked proteins [4,5]. Both ECM organization and composition are organ-dependent and accurately reflect the physiological state, so ECM is substantially altered during neoplasia evolution [6].

Collagen, glycoproteins and proteoglycans are the core components of ECM [4]. Desmoplasia, an excessive deposition of ECM accompanied by aberrant organization and post-translational modifications, is a protumorigenesis event [6,7] and it is usually a signal of poor prognosis and a barrier for chemotherapy. It appears in most solid tumors, particularly in pancreatic ductal adenocarcinoma (PDAC), probably the most stroma-rich tumor [8]. Desmoplasia is characterized by a high collagen content and cross-linking and also by a high collagen turnover due to upregulation of proteolytic enzymes [9], which opens the way to find collagen degradation fragments in the circulation.

All fibril-forming collagens are synthesized as procollagens and contain a central triple helix flanked by two non-helical domains denoted N- and C-telopeptides and the two terminal propeptides at the amino and carboxylic ends (Fig. S1A). Maturation (removal of propeptides) [10] along with proteolytic degradation by matrix metalloproteases and sheddases release small bioactive fragments (matrikines or matrycryptins) and expose peptides hidden in the full-length protein (neopeptides). Some of these collagen fragments have been detected in body fluids, mainly in the blood [11–13] and studied as cancer biomarkers [14].

The description of novel matrikines and neoepitopes as cancer biomarkers must be accompanied by selective probes and sensitive assay formats to evaluate their clinical validity. This is especially urgent for low abundant components such as collagen XI, a minor fibrillar collagen. It presents low expression in normal tissues and is dysregulated in cancers as prevalent as colorectal and breast cancers but also in less common but deadly PDAC [15,16]. Collagen XI is a heterotrimer whose α1 chain (Fig. S1B) presents high level of homology with α1 chain from collagen V, except in the N-propeptide [17]. There are commercial kits using antibodies to detect collagen XI but their selectivity and/or target epitope is not fully disclosed. Interestingly, a mAb specific for a 15-mer peptide from the N-propeptide of α1 chain distinctly stained the peritumoral fibroblasts in PDAC tissues but not normal epithelial, vascular or stromal cells [18]. Very recently, two mAbs targeting two neopeptides arisen from the enzymatic processing of N-propeptide have been obtained to detect the cleaved fragment in the blood as a potential predictive biomarker in PDAC [19]. However, receptors directed to the propeptides fail to discriminate procollagen from mature collagen, the form present in the ECM. Excision of propeptides expose the N- and C-telopeptides, for which there are not specific receptors.

As alternative to antibodies, aptamers are easily selected against a defined epitope or region within a molecule [20] without animal involvement. As single stranded nucleic acids they are chemically and thermally stable and can be combined with nucleic acid amplification strategies to boost sensitivity [21,22]. The *in vitro* selection called SELEX allows aptamer selection in biological media to ensure proper folding and avoid affinity loss, and counter-selection steps to minimize cross-reactivity [23,24].

In this work we describe the selection of the first aptamer for a minor collagen. We used a specific 16mer peptide of the C-telopeptide from human collagen XIα1 (colXIα1) as the target. The obtained aptamers are thoroughly characterized in terms of affinity and selectivity using electrochemical binding assays. ColXIα1 protein has been identified by mass spectrometry from lysates overexpressing the collagen XI but not when an irrelevant DNA sequence was employed after magnetic capture with the winning aptamer D1. Detection of the complete protein using a commercial ELISA kit and the aptamer as indicator probe is demonstrated.

2. Materials and methods

Reagents, instrumentation, and detailed experimental protocols of MBs modification, and cell line culture can be found in the supplementary material.

2.1. SELEX protocol

SELEX was carried out using a single-stranded DNA library of random sequences, whose structure consists of a central region with 40 random nucleotides and two constant regions at the ends that act as a hybridization zone to the PCR primers. The sequences of the DNA library and the PCR primers are indicated in Table S1. As the target, we used a 16-amino acid peptide from collagen XIα1 conjugated to BSA through a cysteine at the N-terminus of the peptide, and we immobilized it on tosylactivated magnetic beads (BSA-16mer-T-MBs). Each round of the SELEX procedure comprised the following steps:

2.1.1. Interaction

In the first round of selection, 1 nmol of the DNA library (23.4 μg) was transferred to a microcentrifuge tube, heated at 98 °C for 5 min,

and immediately cooled on ice for another 5 min. Next, 17.1 μL of BSA-16mer-T-MBs (100 pmol of peptide, for a [DNA]/[peptide] ratio of 10) were added and filled up with 1 × PBS + 1 μg mL^{-1} BSA + 2.34 μg mL^{-1} tRNA to a total volume of 1 mL. BSA was added to the selection medium to avoid nonspecific interactions, while tRNA was used as a competitor to make the selection more stringent. The [DNA]/[tRNA] ratio was kept at a value of 10 throughout all the process. This interaction step between the DNA library and the peptide was carried out at 37 °C for 1 h under continuous shaking (650 rpm).

2.1.2. Partitioning and elution

After each interaction step, the tube was placed on a magnet for 2 min and the supernatant was removed, thus eliminating the unbound DNA. The beads were then washed twice with 500 μL of PBS +0.01% Tween 20. Finally, the bound DNA was eluted with 30 μL of hot ultrapure water, heating at 95 °C for 15 min.

2.1.3. PCR amplification

After the elution, the supernatant (eluate), containing the winning DNA sequences, was collected and amplified by PCR. Each PCR vial (50 μL) contained 2 μL of template (eluate), 1 μM of forward and biotinylated-reverse primers, 0.2 mM dNTPs, 2 mM $MgCl_2$, 1 × reaction buffer, and 2.8 U of DNA polymerase hot-start Immolase™. The mixture was amplified with the following protocol: 95 °C for 10 min; 15 cycles of 1 min at 95 °C, 1 min at 57.5 °C, 1 min at 72 °C; and a final extension at 72 °C for 10 min. The concentration of the generated PCR product was determined using a Qubit™ fluorimeter with the Qubit™ dsDNA HS Assay kit.

After each PCR, the size of the obtained double-stranded DNA (76 bp) was checked by agarose gel electrophoresis, using a DNA size marker of 20 base pairs. In order to do this, a 2% agarose gel was prepared in 1 × TBE buffer pH 8.3 containing 1:10000 of SimplySafe DNA staining dye, that enabled the final visualization of the DNA using UV light. Six μL of size marker and 8–12 μL of a 5:1 mixture of (PCR product):(6 × loading buffer) were loaded onto the gel wells and electrophoresis was run for 45 min applying a potential difference of 110 V.

2.1.4. Conditioning

The recovery of single-stranded DNA, necessary to start a new cycle of selection, was carried out using Dynabeads MyOne™ Streptavidin C1 magnetic beads (strep-MBs). First, the amount of beads required to separate 250 pmol was calculated, taking into account the PCR product concentration, previously measured by fluorimetry (Qubit), and the binding capacity of the particles. The calculated MBs were transferred to a vial and washed 3 times with 500 μL of 5 mM Tris buffer (pH 7.4) + 1 M NaCl + 0.01% Tween 20. Then, the PCR product volume containing 250 pmol was added to the beads and mixed with the same volume of 10 mM Tris (pH 7.4) + 2 M NaCl buffer. The mixture was incubated at room temperatures (RT) for 30 min, with constant stirring. Subsequently, the particles were washed 3 times with 500 μL of 5 mM Tris (pH 7.4) + 1 M NaCl + 0.01% Tween 20 and incubated for 10 min with 50 μL of NaOH 100 mM at 25 °C. In this way, it was possible to denature the DNA duplex, eluting the strand of interest from the beads to the solution, while the complementary strand remained attached to the beads. The resulting supernatant was collected and neutralized with 1 M HCl, to be used as a new DNA pool in the following selection round.

In the second round of selection and onwards, 250 pmol of the starting DNA pool were used instead of 1 nmol, and a counter-selection against BSA was applied. In this step, the DNA library was first incubated with BSA-T-MBs. The supernatant obtained after this interaction, which contained the sequences that did not bind to BSA, was collected, while the sequences that bound to the MBs were discarded. This supernatant was then incubated with the BSA-16mer-T-MBs under the conditions described in Table S2. In this way, the sequences that bound to the peptide-BSA conjugate unspecifically by the BSA moiety and not by the desired peptide region were expelled from the selection process. The stringency of the selection was modified by varying the incubation time, the [DNA]/[peptide] ratio and adding fetal bovine serum (FBS) in the interaction buffer (Table S2).

2.2. Enrichment assay

The evolution of the affinity of the selected sequences was monitored with an enrichment assay, described as follows. First, after heating for 5 min at 98 °C and cooling for 5 min on ice, 25 pmol of ssDNA from each round were incubated with 25 pmol of peptide (BSA-16mer-T-MBs) for 10 min at 37 °C with constant shaking. Afterwards, the supernatant, with the non-binding DNA sequences, was collected, and the beads were washed twice with 500 μL of 1 × PBS + 0.01% Tween 20. Next, the bound DNA was eluted with 30 μL of ultrapure water, heating at 95 °C for 15 min. The concentration of DNA in both fractions, bound and unbound, was measured by UV/Vis absorption spectroscopy at 260 nm, performing an external calibration with the starting DNA library.

2.3. Bradford assay

Total protein concentration in cell lysates and supernatants from magnetic beads modifications was determined by the Bradford assay as follows. 50 μL of blank solution, BSA standards of 0–100 μg mL^{-1} and diluted samples were pipetted into the wells of a microtiter plate in triplicate, followed by the addition of 200 μL of 2:7.5 diluted 5 × Bradford Reagent. The mixture was incubated 5 min at RT and subsequently the absorbance read at 595 nm in a microplate reader. In the case of cell lysates, the solution used for blank, standard preparation, and sample dilution, was 1 × PBS, while in the case of supernatants from magnetic beads modifications, the buffer used was 0.1 M Na-phosphate + 1.2 M $(NH_4)_2SO_4$ without further sample dilution.

2.4. Analysis of the sequences with bioinformatic tools

After cloning and sequencing (detailed protocol in supplementary information), we obtained 47 clones. First, we constructed a phylogenetic tree by multiple sequence alignments with Clustal OMEGA software [25].

Then, recurrent DNA motifs in the sequences were searched running MEME Suite 5.0.5 software [26] with the following settings: motif discovery mode: classic mode; input the primary sequences: type in sequences (FASTA); select the site distribution: zoops (zero or one occurrence per sequence); select the number of motifs: 10.

2.5. Electrochemical binding curves with 16mer-MBs and aptamer-MBs

10 μL of 16mer-MBs (see supplementary information for a detailed protocol of MBs modification) were transferred to a tube and mixed with different concentrations of 6FAM-labeled aptamers in 500 μL of 1 × PBS. After incubating the mixture for 30 min at 37 °C and 650 rpm, the beads were washed twice with 500 μL of 1 × PBS + 0.01% Tween 20 and subsequently reconstituted in 500 μL of antifluorescein-peroxidase (antiF-POD) 0.5 U mL^{-1} in 1 × PBS + 0.5% casein. The enzymatic labeling was performed for 30 min at RT. Next, the MBs were washed again twice with the

surfactant-containing buffer and once with 1 × PBS, and reconstituted in 15 μL of 1 × PBS. All the beads were placed on the working electrode of a carbon screen printed cell (SPCE) and trapped magnetically with the aid of a magnet of the same size as the working electrode, previously stuck under it. Then, the three electrodes of the SPCE were covered with 40 μL of a commercial ready-to-use mixture of TMB and hydrogen peroxide, and the enzymatic reaction was incubated for 1 min at RT. Chronoamperometry at 0 V was carried out immediately after and the generated current was registered for 1 min.

The procedure followed in the assay with the opposite format, that is, aptamer-modified MBs and biotinylated 16mer in solution, was the same, with the only difference being the peroxidase conjugate used. In this second case, the enzymatic labeling was performed with a solution of 2.5 μg mL^{-1} strep-POD prepared in 1 × PBS +0.01% Tween 20.

2.6. Electrochemical binding curves with protein-modified tosylactivated and carboxylated magnetic beads

The protocols to obtain the binding curves with BSA-10/16mer-T-MB, vimentin-C-MBs and BSA-T-MBs (see supplementary information for a detailed protocol of MBs modification) were identical to that of 16mer-MBs in terms of steps and incubation times. The only difference was the amount of modified beads used with each protein, being 3 μL for BSA-16mer and BSA modified T-MBs, 5 μL for BSA-10mer-T-MBs, and 10 μL for vimentin-C-MBs.

2.7. Cell lysate preparation

A-204, NCI−H661 and HT-29 cell lines were cultured (see supplementary information). For cell lysate preparation, the medium in the culture was first replaced by 4 mL of trypsin − EDTA and the cells were incubated in this solution for 2 min in order to detach adherent cells from the flask walls. Subsequently, 4 mL of culture medium were added to the flask to inactivate trypsin, and the cell suspension was collected on a falcon tube and centrifuged for 10 min at 1200 rpm. Finally, the supernatant was removed, and the pellet was washed with PBS and stored at −80 °C. The cells were lysed by the mechanic rupture of their membranes upon freezing and de-freezing steps. Total protein concentration in lysates was determined by the Bradford method as previously described. In some cases, the lysates were centrifuged prior to their use for 20 min at 4 °C and 1500 *g*.

2.8. Cell lysate capture with aptamer-modified magnetic beads

100 μL of aptamer-D1-MB were mixed with 10−15 μL of cell lysate and filled with 1 × PBS up to a volume of 500 μL. After incubating the mixture for 30 min at 37 °C and 650 rpm, the beads were washed twice with 1 × PBS + 0.01% Tween 20. Next, elution of the captured proteins was performed with 50 μL of water at 95 °C for 30 min. The resulting supernatant (purified extract) was collected and further analyzed by SDS-PAGE, LC-MS or ELISA.

2.9. Purified cell lysate analysis by LC-MS

Mass spectrometry analysis of the purified cell extracts obtained after treatment with aptamer-MBs was performed at the Proteomic Unit of the Health Research Institute of Santiago de Compostela (IDIS, Spain). First, the purified cell extracts were subjected to manual tryptic digestion following the protocol defined by Shevchenko et al. [27] with minor modifications: reduction was performed with 10 mM dithiothreitol in 50 mM ammonium bicarbonate and alkylated with 55 mM iodoacetamide in 50 mM ammonium bicarbonate. Then, after drying the samples in a SpeedVac, modified porcine trypsin (Promega, USA) was added at a final concentration of 20 ng μL^{-1} in 20 mM ammonium bicarbonate, and incubated at 37 °C for 16 h. Peptides were extracted three times by 20 min incubation in 40 μL of 60% acetonitrile in 0.5% formic acid. The resulting peptide extracts were pooled, concentrated in a SpeedVac and stored at −20 °C.

Digested peptides were separated using Reverse Phase Chromatography. Gradient was developed using a micro liquid chromatography system (Eksigent Technologies nanoLC 400, SCIEX) coupled to high speed Triple TOF 6600 mass spectrometer (SCIEX) with a micro flow source. The analytical column used was a Chrom XP C18 150 × 0.30 mm, 3 mm particle size and 120 Å pore size (Eksigent, SCIEX). The trap column was a YMC-TRIART C18 (YMC Technologies, Teknokroma) with a 3 mm particle size and 120 Å pore size, switched on-line with the analytical column. The loading pump delivered a solution of 0.1% formic acid in water at 10 μL min^{-1}. The micro-pump provided a flow-rate of 5 μL min^{-1} and was operated under gradient elution conditions, using 0.1% formic acid in water as mobile phase A, and 0.1% formic acid in acetonitrile as mobile phase B. Peptides were separated using a 15 min gradient ranging from 2% to 90% mobile phase B (mobile phase A: 2% acetonitrile, 0.1% formic acid; mobile phase B: 100% acetonitrile, 0.1% formic acid). Injection volume was 4 μL (4 μg of sample).

Data acquisition was carried out in a TripleTOF 6600 System (SCIEX, Foster City, CA) using a Data dependent workflow. Source and interface conditions were as follows: ionspray voltage floating (ISVF) 5500 V, curtain gas (CUR) 25, collision energy (CE) 10 and ion source gas 1 (GS1) 25. Instrument was operated with Analyst TF 1.7.1 software (SCIEX, USA). Switching criteria was set to ions greater than mass to charge ratio (m/z) 350 and smaller than m/z 1400 with charge state of 2−5, mass tolerance 250 ppm and an abundance threshold of more than 200 counts (cps). Former target ions were excluded for 15 s. Instrument was automatically calibrated every 4 h using as external calibrant tryptic peptides from pepcalMix.

After MS/MS analysis, data files were processed using ProteinPilot™ 5.0.1 software from Sciex which uses the algorithm Paragon™ for database search and Progroup™ for data grouping. Data were searched using Human specific Uniprot database. False discovery rate was performed using a non-lineal fitting method displaying only those results that reported a 1% global false discovery rate or better [28,29].

3. Results and discussion

3.1. Selection of aptamers for 16-mer C-telopeptide

The target region of the α1 chain is the proteolytic site of the C-propeptide that is expected to be processed to generate the mature form by analogy to the collagen V maturation [30]. We selected a 16mer peptide as the target that was conjugated to BSA (BSA-16mer). This conjugate was anchored on tosylactivated magnetic beads (see supplementary information). This ensures an adequate exposition of the target and facilitate the access of the DNA library. In fact, when the 16mer was directly bound to strep-MBs, no significant enrichment was observed at least after a few rounds of selection. The modified MBs (BSA-16mer-T-MBs) were incubated with the initial library (Fig. 1). The incubation time and the DNA to peptide ratio were varied each round to increase the stringency of the selection (Table S2).

The first round omitted the negative selection but, starting in round 2, a step using BSA-T-MBs (no target) was added to avoid the enrichment in sequences with affinity for the support or the carrier protein. The supernatant of the interaction with BSA-T-MBs,

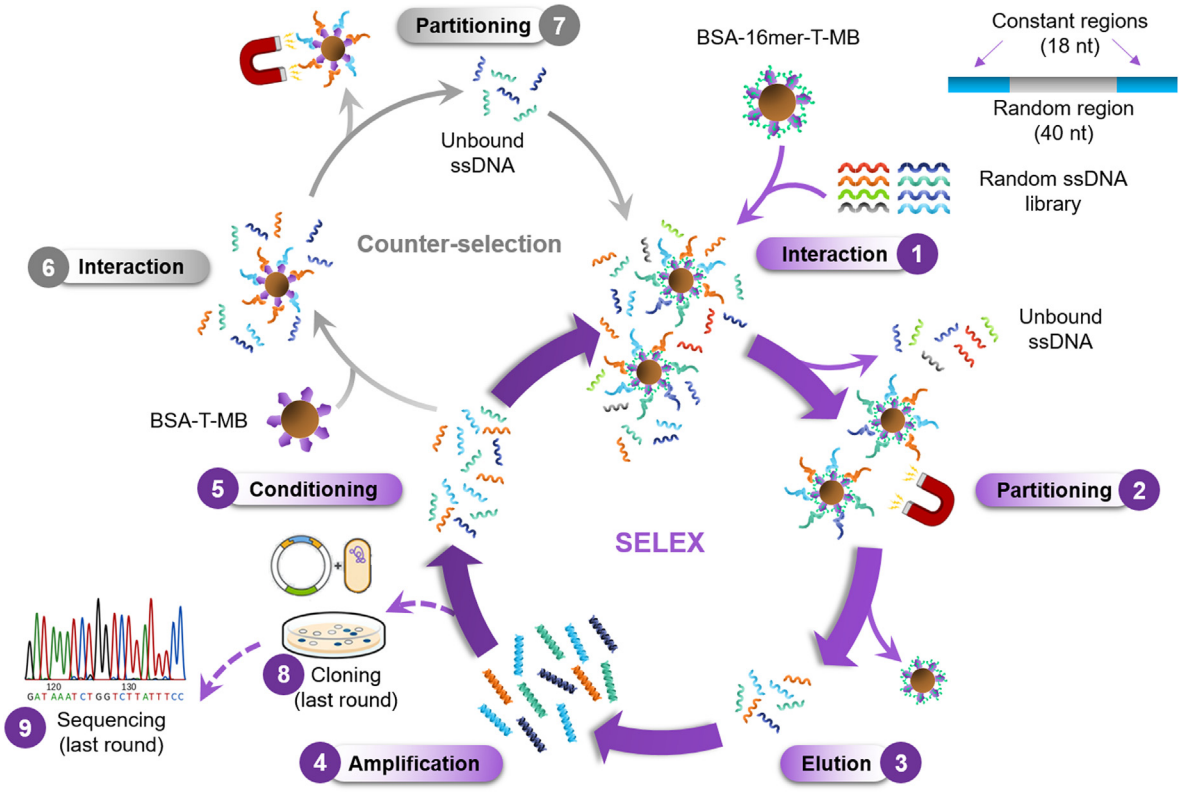

Fig. 1. Schematic depiction of the SELEX procedure used in this work including all the steps: 1 interaction with target-modified MBs, 2 partitioning, 3 elution, 4 amplification, 5 conditioning, 6 interaction with non-target modified MBs (counter selection) 7 partitioning of the counter-selection, 8 cloning and 9 sequencing.

containing the sequences that do not bind to the solid support, was immediately used for the next positive selection with BSA-16mer-T-MBs. In round 5, 5% of FBS was added to the selection buffer to mimic the physiological conditions.

To evaluate the enrichment, each round pool was incubated with the BSA-16mer-T-MBs, and the bound and unbound fractions were quantified by UV/Vis spectroscopy at 260 nm. The percentage of the bound fraction increased up to round 4 (47%) and then decreased (Fig. 2A), indicating that more stringent conditions did not improve the affinity. In our experience, enrichments from above 12% [31–33] can be considered successful, so the 4th round was cloned and sequenced.

The primers regions were trimmed before the *in-silico* analysis. Participation of primers in the binding is rare because strong secondary structures involving the primer regions are more difficult to amplify by PCR and they finally disappear from the pool after several rounds [34]. When the 44 candidates were grouped by sequence homology (Fig. S2) and analyzed for recurrent short motifs using the appropriate software, we found 8 motifs repeated in more than one sequence (Fig. S3). The refined selection of sequences was based on the number of motifs presented, covering all of them, and the thermodynamic stability of the secondary structure (estimated with mfold web server [35]). Nine sequences were selected (B2, B3, C1, C2, C10, D1, D8, G8, H1) whose structures and Gibbs energy values can be seen in Fig. S4. All of them contain two motifs except D8 that only have the motif that always appears alone (the light green motif), and G8 and H1, which were selected because of their stable secondary structure.

3.2. Aptamer screening and characterization

To test the recognition of the 16mer peptide, the nine sequences selected were synthesized with a 6-carboxyfluorescein label separated from the main sequence by a 5-thymine spacer at 5' end (6FAM-apt). 500 nM of each aptamer was incubated with BSA-16mer-T-MBs and then labeled with the enzyme conjugate. After addition of the substrate, the cathodic current was recorded. All aptamers showed affinity for the target but the blank-subtracted current was much higher for H1, G8, D1 and C1 (Fig. 2B). In these four sequences, the light blue [C(C/A)(C/G)(G/T)CGGC] and pink [CA(C/A)A(A/C)G(T/C)G(C/G)TACC] motifs appear twice; alone (G8 and H1) or combined with other motifs (D1 and C1), suggesting that they are important for binding. These four aptamers were characterized in more detail.

First of all, the ability of the aptamers to capture the peptide in solution was tested. The biotinylated aptamers were immobilized on strep-MBs and incubated with increasing concentrations of the biotinylated 16mer. The current recorded was used to plot the binding curves, *I* vs peptide concentration. They were fitted to the Langmuir model, which involves 1:1 interaction, to calculate the dissociation constant (K_d) (Fig. 3A, B and S5). In this configuration, D1 showed the best K_d (247 ± 79 nM), about 6-fold smaller than C1 (1598 ± 136 nM), 7.5-fold than H1 (1871 ± 270 nM) and 8-fold than G8 (1975 ± 190 nM).

Both D1 and C1 were assayed in the reversed configuration. Binding curves were constructed with increasing concentrations of each 6FAM-aptamer incubated with biotinylated 16-mer immobilized on strep-MBs. These plots best fitted to the Hill model, with slightly positive cooperativity (Hill coefficient: $n > 1$). The K_d values were identical (about 25 nM), which is 1 and 2.5 orders of magnitude smaller than in the former configuration for D1 and C1, respectively (Fig. 3C and D). The improved affinity constant might be a consequence of a "surface effect" that facilitates rebinding of the aptamer before diffusing away from the particle due to the high

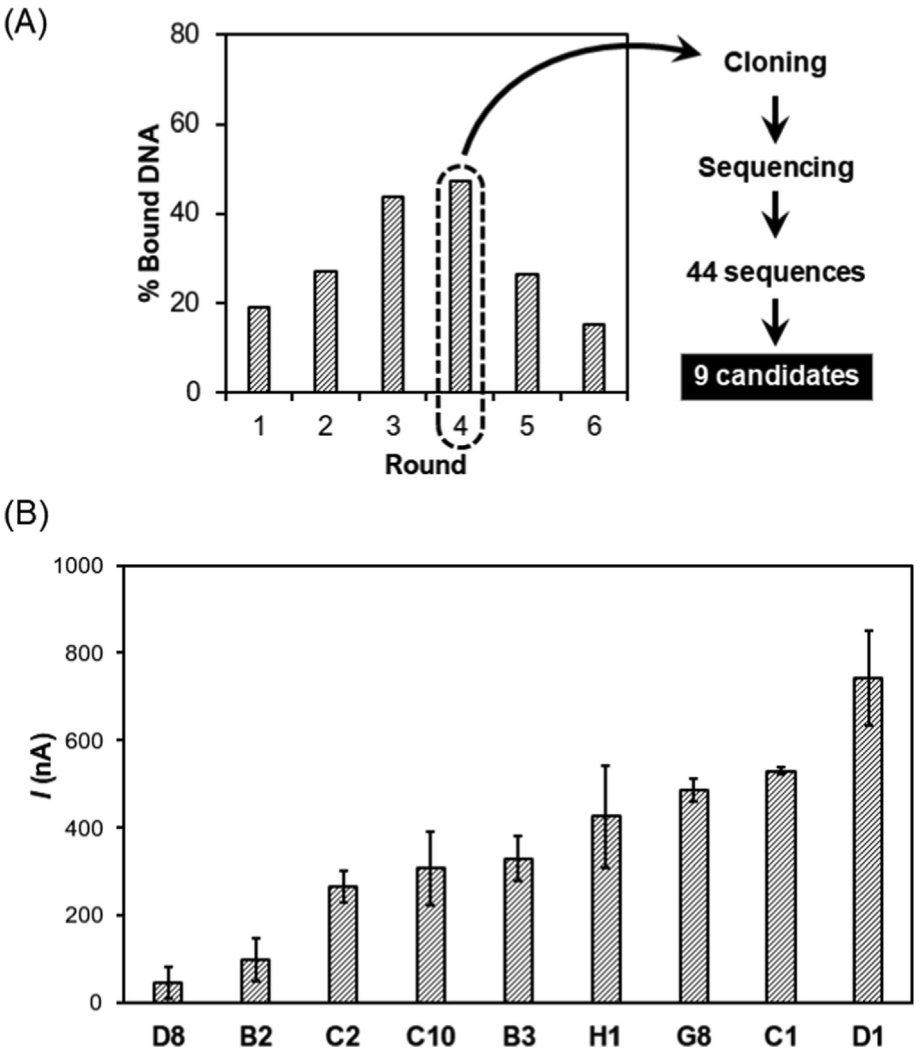

Fig. 2. A) Enrichment assay: percentage of DNA from each SELEX round that binds to the BSA-16mer-T-MBs as measured by UV/Vis spectroscopy at 260 nm. B) Affinity screening: Direct binding assay using the BSA-16mer-T-MBs (20 μg) and 500 nM of each 6FAM-aptamer candidate in solution. Currents were measured chronoamperometrically at 0 V after addition of the enzyme conjugate and 1 min of reaction with the TMB + H_2O_2 substrate.

target coverage [36]. As a result, an apparent smaller dissociation rate constant and a smaller apparent K_d are obtained. Steric hindrance between aptamers on the surface or accessibility of the peptide cannot be discarded as a plausible explanation for the decreased binding of the peptide to the immobilized aptamers [37]. Overall, the aptamer D1 is the sequence with the best performance in both configurations and was used in further experiments.

3.3. Identification of the "aptatope"

Typical antibody linear epitopes usually comprise less than 10 amino acids [38]. For this reason, we challenged the D1 aptamer to a truncated peptide version without the six C-terminal amino acids. The 10mer peptide was conjugated to BSA (BSA-10mer) and immobilized on T-MBs as carried out with the BSA-16mer. The binding curve was obtained using 100 μg of modified MBs and increasing concentrations of 6FAM-D1 (Fig. 4A). The aptamer binds to both peptides and the currents are much higher for the 10mer indicating that the truncated hexamer is not essential for binding.

Accordingly, the binding constant is much smaller (250 ± 33 nM) for BSA-10mer than for BSA-16mer (5.7 ± 6.4 μM), so the decapeptide is the actual "aptatope". The saturation is not achieved with BSA-16mer, which makes the estimation of K_d less reliable and can account for the discrepancy with the K_d value calculated when the biotinylated peptide was immobilized. Curiously, cooperativity was only observed with 10mer (n = 1.8 ± 0.3 vs n = 0.97 ± 0.07), which also agrees with the higher currents measured. To the best of our knowledge, there is only one aptamer developed against a C-telopeptide. In that case, the target was a 26mer fragment of the α1 chain of the major collagen I. As in our case, the aptatope was the innermost part of the peptide because the terminal octapeptide did not bind to it [39].

3.4. Selectivity

The selection of undesired aptamers with affinity for the target carrier (BSA) was minimized with the negative selection steps. The success of this strategy was verified incubating the 6FAM-D1 aptamer with BSA-T-MBs and measuring the bound aptamer electrochemically. The chronoamperometric currents were about 72% smaller than those obtained when challenging the aptamer to 16mer-MBs (Fig. 4B). The specific binding of D1 aptamer to 16mer peptide in solution was also confirmed in a blocking assay. 16mer-MBs were incubated with increasing concentrations of 6FAM-D1

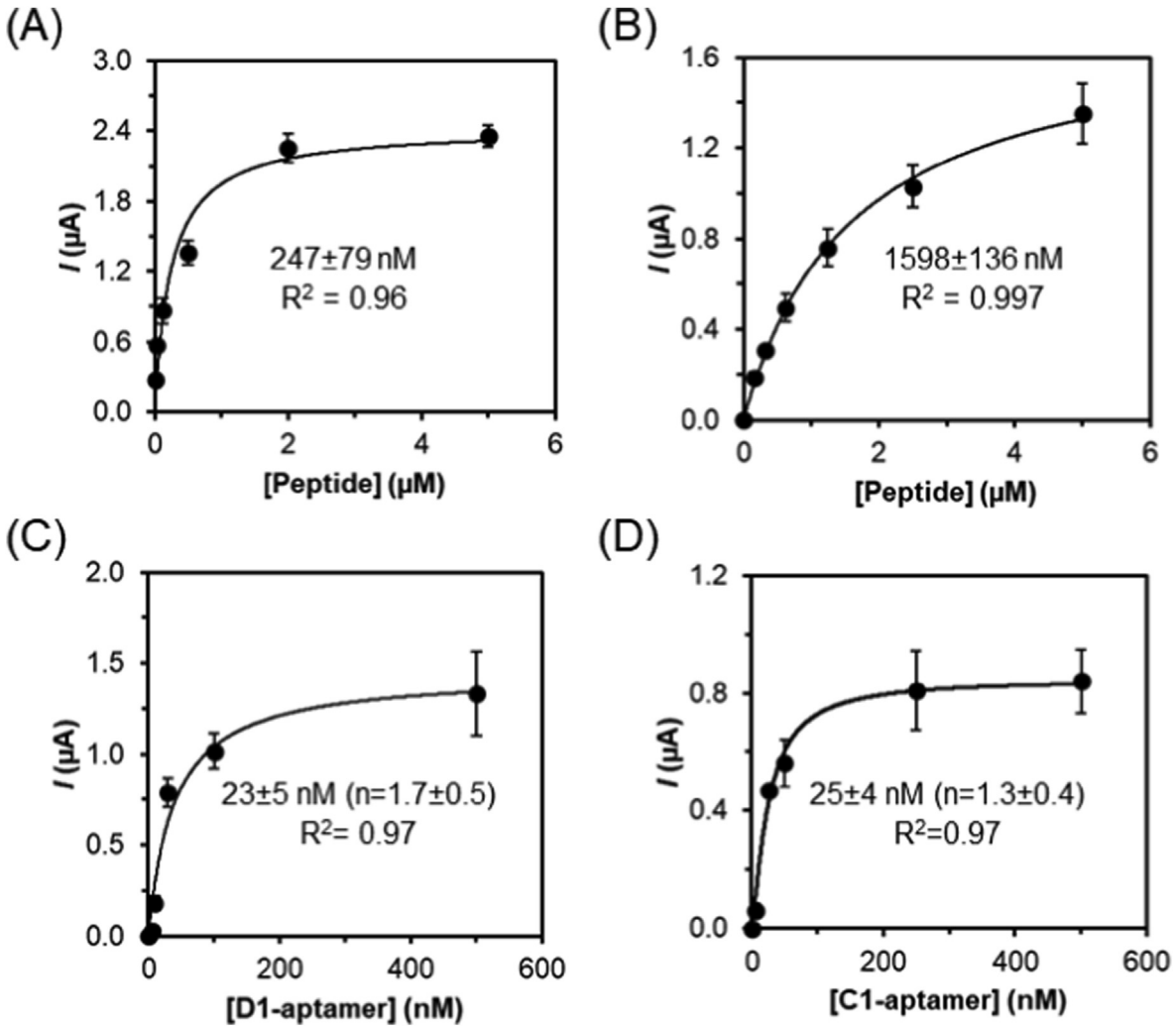

Fig. 3. Characterization of the best aptamer candidates; D1 (A and C) and C1 (B and D) by electrochemical binding assays on two different configurations. In A and B, the biotinylated aptamers were immobilized on strep-MBs and the biotinylated 16mer peptide was increasingly added in solution. In C and D, the biotinylated 16mer was immobilized on the strep-MBs and the 6FAM-aptamer was added in solution. The affinity constant value (K_d) calculated by curve fitting to Langmuir or Hill model is also indicated. Measurement conditions as in Fig. 2.

aptamer with or without 1 μM of the peptide in solution (Fig. 4B). In the presence of the peptide, the current measured is about 80% smaller than in its absence. This means that the formation of the aptamer-16-mer complex in solution takes places and effectively competes with the binding on the surface.

The specific binding of the target in biological matrices was also investigated using two colXIα1 positive cell lines (A-204 and NCI−H661) and a negative control (HT-29) (Table S3). 80 μg of protein of each lysate (measured by Bradford method for normalization) was incubated with a fixed amount of aptamer-D1-MBs. The bound fraction was eluted and analyzed by SDS-PAGE. It reveals a distinct band at about 55 kDa for A-204 cells that is not visible in the other two cell types (Fig. S6). This band was isolated and analyzed by LC-MS after trypsin digestion. 42 proteins were identified at 99% confidence level (supplementary file). The protein with the highest number of peptides and total coverage was vimentin (128 peptides and 77.9% coverage), an intermediate filament with a 57 kDa MW that is a marker of the epithelial-to-mesenchymal transition (EMT) [40]. Since the A-204 is a mesenchymal line the expression of vimentin is expected to be higher than in NCI−H661 cell line, which is a tumor-transformed epithelial cell. Interestingly, several blind cell-SELEX (not defined target) have identified the vimentin as the unexpected target by LC-MS [41,42].

Electrochemical binding assays show that D1 aptamer did bind to vimentin but the affinity is lower than for 16mer. We modified C-MBs with vimentin and incubated them with increasing concentrations of 6FAM-D1 aptamer. Though the amount of vimentin theoretically immobilized on the particles (21 pmol) is larger than the amount of the 16mer peptide (8 pmol) the currents are much smaller, indicating lower amount of aptamer bound to the surface. This result agrees with a higher K_d, 173 ± 53 nM.

As vimentin is involved in EMT, it is reasonable to hypothesize that vimentin concentration in the lysate might be higher than that of collagen XI. This could shift the equilibrium toward the vimentin binding despites the inferior affinity. To try to eliminate this interference, the lysates were centrifuged to remove cell debris before incubating the supernatant with the aptamer on MBs. The analysis of the eluted fraction by SDS-PAGE showed the disappearance of the distinct band associated with vimentin (Fig. S6, bottom panel). The centrifuged and aptamer-treated lysate was analyzed by LC-MS as indicated above. Under these conditions 53 proteins were identified. Among them vimentin is still present but only with 24 peptides and a lower coverage (41%). Collagen XI was also identified with one peptide at the 99% confidence level.

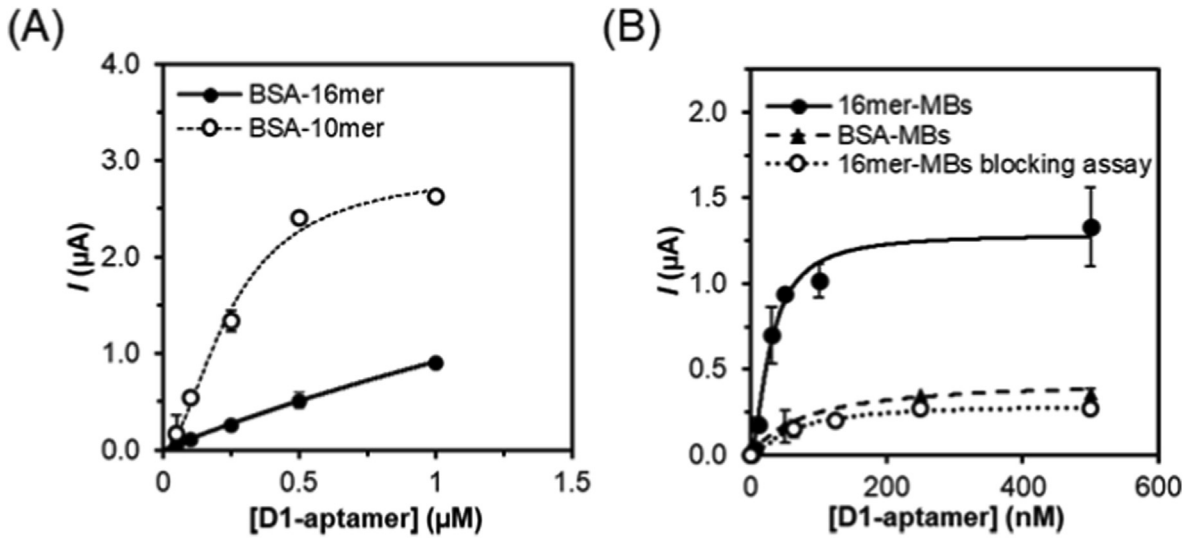

Fig. 4. Selectivity of 6FAM-D1 aptamer. A) Binding curve to BSA-10mer (white circle) and BSA-16mer (black circle) immobilized on T-MBs (100 μg). B) Binding curves to biotinylated 16mer on strep-MBs in the absence (black circle) and in the presence (white circles) of 16-mer peptide in solution (blocking assay), and to BSA-T-MBs (no peptide in solution) (black triangles). Measurement conditions as in Fig. 2.

Control experiments using an irrelevant DNA sequence (T40) immobilized on strep-MBs showed a weaker band at about 55 kDa, only for A-240 when the lysates were not centrifuged (Fig. S6). This result suggests that the presence of vimentin in the eluted fraction is not only due to some cross-reactivity of D1 aptamer but also to the unspecific binding to the MBs. LC-MS analysis of the centrifuged lysate from A-240 after exposure to T40-MB identified 183 proteins. Venn diagram of proteins identified after D1 and T40 entrapment shows only 11 proteins that exclusively appears in D1 treated sample, among them the collagen XI (Fig. S7). Vimentin along with other 41 proteins appear in both samples. This observation indicates that the unspecific interaction with the MBs dominates the population of eluted proteins.

3.5. Evaluation of the peptide recognition within the protein

We wanted to know whether the aptamer recognizes the peptide within the complete protein in a dose-dependent manner. However, there is no standard for collagen XI, so we decided to use the cell lysates as a source of target and evaluate the aptamer recognition using commercial ELISA kits (Table S4). First of all, we examine the target of each kit to avoid shared epitopes that prevent simultaneous detection between capture antibody and aptamer. Cusabio kit does not inform about the targeted fragment used as the standard while Cloud-Clone and Elabscience kits targeted a peptide from the C-propeptide (1564–1806) and from the mature collagen (738–985), respectively. In principle, there is no overlapping but Cloud-Clone kit does not detect the mature collagen.

We tested the cross-reactivity by assaying the centrifuged cell lysates with and without purification with the D1 aptamer. All three kits use a biotinylated antibody for detection that is further labeled with an avidin-POD conjugate. Cusabio kit was discarded because we obtained very high absorbances in the absence of the secondary antibody indicating that the enzymatic conjugate adsorbs unspecifically. The CloudClone kit was unable to detect collagen XI in the A-204 lysate, which is expected to highly express the target, and only a small concentration is found after aptamer preconcentration with D1 (Table 1). Unexpectedly, the concentration in NCI–H661 (+) was higher and clearly decreases after aptamer purification, which suggests strong cross-reactivity, as was confirmed with the negative cell-line, for instance with collagen V. The manufacturer was unable to rule out completely any interference from analogue. Since the target of the kit is the C-propeptide, this result may be explained if procollagen is the dominant form, and the aptamer target (the C-telopeptide) is hidden; so, only after processing, the aptatope would be unveiled and available for aptamer capture.

On the contrary, Elabscience kit showed higher collagen XI concentrations in the A-204 lysate than in NCI–H661 after aptamer purification. An enrichment factor of 6 is estimated in A-204 cell line while only 1.6 in the NCI–H661, which would correlate with an increased expression of the mature collagen. The detection of collagen XI even after purification in the HT-29 also points to some kind of cross reactivity even though the capture antibody is monoclonal.

Elabscience kit was selected to detect the mature collagen XI in the lysates in a mixed sandwich assay using the capture mAb and the D1 aptamer as detection receptor. Since we obtained aptamers for a short peptide, a sandwich assay with two aptamers is not possible for steric reasons. Quantitation was not performed because the standards do not contain the aptatope (the C-telopeptide). The results were compared with those obtained with the immunoassay in terms of the analytical signal (Table 2). In general, the aptamer assay provides larger analytical signals than the antibody. Of note, these high signals cannot be attributed to vimentin. We tested the immunoassay with vimentin and no absorbance was measured indicating that antibodies do not crosstalk with it. The blank experiments, without sample, using the D1 aptamer show a readout of ~0.1 u.a, so interaction with the microplate or with the capture mAb is not the cause. We attribute the high signals to the use of a streptavidin-POD conjugate instead of the avidin conjugate employed to label the antibody. Streptavidin presents lower unspecific binding due to its lower pI but it contains a tripeptide that mimics the universal RGD receptor of fibronectin and other adhesion molecules [43]. Those molecules are present in the cell lysate and can unspecifically bind to the MBs. If this happens streptavidin but not avidin might bind to them. The kit manufacturer declares that there is not cross-reactivity between collagen XIα1 and its analogues but some cross-reactivity may still exist.

In both assays the trend is similar; the highest absorbances were obtained for A-204 lysate followed by NCI–H661 and the negative

Table 1
Concentration of colXIα1 in the cell lysates using two different commercial kits with and without purification with D1-aptamer. Standard deviations correspond to n = 2 as indicated in the kit.

Sample	Cloud-Clone kit	Elabscience kit
	pg colXIα1 mg^{-1} protein	
A-204 (centrifuged lysate)	< LD	98 ± 10
A-204 (D1-purified lysate)	12 ± 2	596 ± 57
A-204 (D1-purified without prior centrifugation)	Not tested	307 ± 29
NCI−H661 (centrifuged lysate)	125 ± 12	121 ± 13
NCI−H661 (D1-purified lysate)	9 ± 1	193 ± 19
HT-29 (centrifuged lysate)	270 ± 26	200 ± 19
HT-29 (D1-purified lysate)	80 ± 8	180 ± 17

Table 2
Absorbances obtained with the Elabscience kit using the pAb or D1-aptamer as detection receptor for the three cell centrifugated lysates after purification with D1 aptamer. Standard deviations correspond to n = 2 as indicated in the kit.

Sample	pAb	D1
	Abs (u.a.)	
A-204	0.532 ± 0.095	0.880 ± 0.099
NCI−H661	0.353 ± 0.033	0.482 ± 0.056
HT -29	0.246 ± 0.013	0.316 ± 0.037

cell line HT-29. These results confirm that D1 aptamer is a promising receptor for the detection of collagen XIα1 in biological media.

4. Conclusions

The availability of selective receptors is critical to the development of simple assays to establish the clinical utility of novel cancer biomarkers. The lack of them for ECM components is outstanding, especially for collagens, large proteins with a high sequence homology. In this work we have obtained aptamers for the detection of a specific peptide that is supposed to be exposed after collagen release into the ECM and maturation. After screening through electrochemical direct assays, D1 aptamer showed the best performance with a K_d of about 25 nM. Mass spectrometry measurements confirmed that the aptamer captures this minor collagen in cell lysates, which indicates that it is not degraded or losing affinity in complex media. Besides, the D1 aptamer was able to detect the collagen from the lysates in a sandwich assay using an antibody for capture. We envisage the design of competitive assays based only on aptamers for the detection of the soluble fragment in biological fluids.

CRediT authorship contribution statement

Ramón Lorenzo-Gómez: Methodology, Investigation, Data curation, Writing − original draft, Writing − review & editing. **Rebeca Miranda-Castro:** Supervision, Conceptualization, Methodology, Writing − review & editing. **Juan R. de los Toyos:** Conceptualization, Supervision, Writing − review & editing. **Noemí de-los-Santos-Álvarez:** Conceptualization, Supervision, Data curation, Methodology, Writing − original draft, Writing − review & editing. **María Jesús Lobo-Castañón:** Conceptualization, Resources, Project administration, Supervision, Writing − review & editing.

Declaration of competing interest

The authors declare that they have no known competing financial interests or personal relationships that could have appeared to influence the work reported in this paper.

Acknowledgements

This research was funded by the Spanish Government (project RTI-2018-095756-B-I00). RLG. thanks the Spanish Government for a PhD fellowship (FPU16/05670). We also thank Dr. M. García Ocaña for his help and guidance in the experiments with cells, as well as the Sequencing Unit from the Scientific and Technological Resources of the University of Oviedo, where PCR, electrophoresis, cloning and sequencing experiments were performed, and the Proteomic Unit from the Health Research Institute of Santiago de Compostela (IDIS), where mass spectrometry analyses were carried out.

Appendix A. Supplementary data

Supplementary data to this article can be found online at https://doi.org/10.1016/j.aca.2021.339206.

References

[1] G. Rossi, M. Ignatiadis, Promises and pitfalls of using liquid biopsy for precision medicine, Cancer Res. 79 (2019) 2798−2804.
[2] J. Wu, et al., Tumor circulome in the liquid biopsies for cancer diagnosis and prognosis, Theranostics 10 (2020) 4544−4556.
[3] E. Henke, R. Nandigama, S. Ergün, Extracellular matrix in the tumor microenvironment and its impact on cancer therapy, Front. Mol. Biosci. 6 (2020) 160.
[4] A. Naba, K.R. Clauser, S. Hoersch, H. Liu, S.A. Carr, R.O. Hynes, The matrisome: in silico definition and in vivo characterization by proteomics of normal and tumor extracellular matrices, Mol. Cell. Proteomics 11 (2012), M111.014647.
[5] R.O. Hynes, The extracellular matrix: not just pretty fibrils, Science 326 (2009) 1216−1219.
[6] M.W. Pickup, J.K. Mouw, V.M. Weaver, The extracellular matrix modulates the hallmarks of cancer, EMBO Rep. 15 (2014) 1243−1253.
[7] N. Willumsen, N.I. Nissen, M.A. Karsdal, The roles of collagens in cancer, in: M.A. Karsdal (Ed.), Biochemistry of Collagens, Laminins and Elastin, second ed., Academic Press, 2019, pp. 341−352.
[8] M.A. Shields, S. Dangi-Garimella, A.J. Redig, H.G. Munshi, Biochemical role of the collagen-rich tumour microenvironment in pancreatic cancer progression, Biochem. J. 441 (2011) 541−552.
[9] K. Kessenbrock, V. Plaks, Z. Werb, Matrix metalloproteinases: regulators of the tumor microenvironment, Cell 141 (2010) 52−67.
[10] H.P. Bächinger, K. Mizuno, J.A. Vranka, S.P. Boudko, Collagen formation and structure, in: H.-W. Liu, L. Mander (Eds.), Comprehensive Natural Products II, Elsevier, Oxford, 2010, pp. 469−530.
[11] A. Lipton, et al., High turnover of extracellular matrix reflected by specific protein fragments measured in serum is associated with poor outcomes in two metastatic breast cancer cohorts, Int. J. Cancer 143 (2018) 3027−3034.
[12] D.P. Hurkmans, C. Jensen, S.L.W. Koolen, J. Aerts, M.A. Karsdal, R.H.J. Mathijssen, N. Willumsen, Blood-based extracellular matrix biomarkers are correlated with clinical outcome after PD-1 inhibition in patients with metastatic melanoma, J. Immunother. Cancer 8 (2020), e001193.
[13] Y.-Q. Luo, et al., Development of an ELISA for quantification of tumstatin in serum samples and tissue extracts of patients with lung carcinoma, Clin. Chim. Acta 411 (2010) 510−515.
[14] R. Lorenzo-Gómez, R. Miranda-Castro, N. de-los-Santos-Álvarez, M.J. Lobo-Castañón, Bioanalytical methods for circulating extracellular matrix-related proteins: new opportunities in cancer diagnosis, Anal. Bioanal. Chem. (2021), https://doi.org/10.1007/s00216-021-03416-2 in press.
[15] Z. Raglow, S.M. Thomas, Tumor matrix protein collagen XIα1 in cancer, Cancer Lett. 357 (2015) 448−453.

[16] C. García-Pravia, et al., Overexpression of COL11A1 by cancer-associated fibroblasts: clinical relevance of a stromal marker in pancreatic cancer, PLoS One 8 (2013), e78327.
[17] M. García-Ocaña, et al., Characterization of a novel mouse monoclonal antibody, clone 1E8.33, highly specific for human procollagen 11A1, a tumor-associated stromal component, Int. J. Oncol. 40 (2012) 1447–1454.
[18] J.A. Galván, et al., Validation of COL11A1/procollagen 11A1 expression in TGF-β1-activated immortalised human mesenchymal cells and in stromal cells of human colon adenocarcinoma, BMC Cancer 14 (2014) 867.
[19] N.I. Nissen, et al., Noninvasive prognostic biomarker potential of quantifying the propeptides of Type XI collagen alpha-1 chain (PRO-C11) in patients with pancreatic ductal adenocarcinoma, Int. J. Cancer 149 (2021) 228–238.
[20] A. Díaz-Fernández, R. Miranda-Castro, N. Díaz, D. Suárez, N. de-los-Santos-Álvarez, M.J. Lobo-Castañón, Aptamers targeting protein-specific glycosylation in tumor biomarkers: general selection, characterization and structural modeling, Chem. Sci. 11 (2020) 9402–9413.
[21] R. Lorenzo-Gómez, R. Miranda-Castro, N. de-los-Santos-Álvarez, M.J. Lobo-Castañón, Electrochemical aptamer-based assays coupled to isothermal nucleic acid amplification techniques: new tools for cancer diagnosis, Curr Opin Electrochem 14 (2019) 32–43.
[22] F. Li, H. Zhang, Z. Wang, A.M. Newbigging, M.S. Reid, X.F. Li, X.C. Le, Aptamers facilitating amplified detection of biomolecules, Anal. Chem. 87 (2015) 274–292.
[23] A. Díaz-Fernández, R. Lorenzo-Gómez, R. Miranda-Castro, N. de-los-Santos-Álvarez, M.J. Lobo-Castañón, Electrochemical aptasensors for cancer diagnosis in biological fluids – a review, Anal. Chim. Acta 1124 (2020) 1–19.
[24] L. Wu, et al., Aptamer-based detection of circulating targets for precision medicine, Chem. Rev. 121 (2021) 12035–12105.
[25] F. Sievers, et al., Fast, scalable generation of high-quality protein multiple sequence alignments using Clustal Omega, Mol. Syst. Biol. 7 (2011) 539.
[26] T.L. Bailey, et al., MEME SUITE: tools for motif discovery and searching, Nucleic Acids Res. 37 (2009) W202–W208.
[27] A. Shevchenko, M. Wilm, O. Vorm, M. Mann, Mass spectrometric sequencing of proteins from silver-stained polyacrylamide gels, Anal. Chem. 68 (1996) 850–858.
[28] I.V. Shilov, et al., The Paragon algorithm, a next generation search engine that uses sequence temperature values and feature probabilities to identify peptides from tandem mass spectra, Mol. Cell. Proteomics 6 (2007) 1638–1655.
[29] W.H. Tang, I.V. Shilov, S.L. Seymour, Nonlinear fitting method for determining local false discovery rates from decoy database searches, J. Proteome Res. 7 (2008) 3661–3667.
[30] E. Kessler, A. Fichard, H. Chanut-Delalande, M. Brusel, F. Ruggiero, Bone morphogenetic protein-1 (BMP-1) mediates C-terminal processing of procollagen V homotrimer, J. Biol. Chem. 276 (2001) 27051–27057.
[31] S. Amaya-González, N. de-los-Santos-Álvarez, A.J. Miranda-Ordieres, M.J. Lobo-Castañón, Aptamer binding to celiac disease-triggering hydrophobic proteins: a sensitive gluten detection approach, Anal. Chem. 86 (2014) 2733–2739.
[32] R. Svigelj, N. Dossi, R. Toniolo, R. Miranda-Castro, N. de-los-Santos-Álvarez, M.J. Lobo-Castañón, Selection of anti-gluten DNA aptamers in a deep eutectic solvent, Angew. Chem. Int. Ed. 57 (2018) 12850–12854.
[33] A. Díaz-Fernández, R. Miranda-Castro, N. de-los-Santos-Álvarez, E. Fernández Rodríguez, M.J. Lobo-Castañón, Focusing aptamer selection on the glycan structure of prostate-specific antigen: toward more specific detection of prostate cancer, Biosens. Bioelectron. 128 (2019) 83–90.
[34] T. Wang, C. Chen, L.M. Larcher, R.A. Barrero, R.N. Veedu, Three decades of nucleic acid aptamer technologies: lessons learned, progress and opportunities on aptamer development, Biotechnol. Adv. 37 (2019) 28–50.
[35] M. Zuker, Mfold web server for nucleic acid folding and hybridization prediction, Nucleic Acids Res. 31 (2003) 3406–3415.
[36] Y. Wu, R.D. Tilley, J.J. Gooding, Challenges and solutions in developing ultrasensitive biosensors, J. Am. Chem. Soc. 141 (2019) 1162–1170.
[37] C. Daniel, Y. Roupioz, D. Gasparutto, T. Livache, A. Buhot, Solution-phase vs surface-phase aptamer-protein affinity from a label-free kinetic biosensor, PLoS One 8 (2013), e75419.
[38] L. Berglund, J. Andrade, J. Odeberg, M. Uhlén, The epitope space of the human proteome, Protein Sci. 17 (2008) 606–613.
[39] J.G. Bruno, M.P. Carrillo, T. Phillips, D. Hanson, J.A. Bohmann, DNA Aptamer beacon assay for C-telopeptide and handheld fluorometer to monitor bone resorption, J. Fluoresc. 21 (2011) 2021.
[40] D. Frescas, et al., Senescent cells expose and secrete an oxidized form of membrane-bound vimentin as revealed by a natural polyreactive antibody, Proc. Natl. Acad. Sci. Unit. States Am. 114 (2017) E1668–E1677.
[41] G.S. Zamay, et al., Aptamers selected to postoperative lung adenocarcinoma detect circulating tumor cells in human blood, Mol. Ther. 23 (2015) 1486–1496.
[42] S. Yoon, B. Armstrong, N. Habib, J.J. Rossi, Blind SELEX approach identifies RNA aptamers that regulate EMT and inhibit metastasis, Mol. Cancer Res. 15 (2017) 811–820.
[43] R. Alon, E.A. Bayer, M. Wilchek, Streptavidin contains an RYD sequence which mimics the RGD receptor domain of fibronectin, Biochem. Biophys. Res. Commun. 170 (1990) 1236–1241.